Chalcogenide Letters Vol. 11, No. 4, April 2014, p. 189 - 197

GROWTH OPTIMIZATION OF ZnS THIN FILMS BY RF MAGNETRON SPUTTERING AS PROSPECTIVE BUFFER LAYER IN THIN FILM SOLAR CELLS

F. HAQUE[a], K. S. RAHMAN[a], M. A. ISLAM[a], M. J. RASHID[a], M. AKHTARUZZAMAN[a], M. M. ALAM[c], Z. A. ALOTHMAN[c], K. SOPIAN[a], N. AMIN[a,b,c*]

[a]*Solar Energy Research Institute, The National University of Malaysia, 43600 Bangi, Selangor, Malaysia*

[b]*Department of Electrical, Electronic and Systems Engineering, Faculty of Engineering and Built Environment, The National University of Malaysia, 43600 Bangi, Selangor, Malaysia*

[c]*Advanced Materials Research Chair, Chemistry Department, College Of Sciences, King Saud University, Riyadh 11451, Kingdom Of Saudi Arabia*

ZnS thin films were grown on soda lime glass substrates by RF Magnetron sputtering technique at room temperature. Deposited films were annealed at 300˚C, 400˚C & 500˚C for 40 minutes, respectively. A comparative study of the structural, optical and electrical properties of the as-deposited and annealed samples was executed through XRD, AFM, UV-VIS spectrometry and Hall Effect measurement. From XRD, it has been found that the as-deposited films are amorphous in nature, whereas the significant peaks of the annealed samples reflects better crystallinity with (111) preferential orientation around 2θ=28.88˚. The surface roughness of the films is also highly affected by the annealing temperature as observed from the AFM images. The optical properties of the films were ascertained for the photon wavelength ranging from 300 to 900 nm. The bandgaps of the films were found in the range of 3.19 eV to 3.29 eV. From the electrical characterization, bulk carrier density is found to be in the range of $10^{12}/cm^3$. The values of resistivity, mobility, Hall coefficient of the films are found to change significantly for different annealing temperatures.

(Received March 6, 2014; Accepted April 11, 2014)

Keywords: ZnS thin films, Magnetron sputtering, Annealing, XRD, AFM, Optical bandgap, Hall Effect measurement.

1. Introduction

To date, in thin film solar cells, CdS has been the most common II-VI compound n-type semiconductor used as a buffer/window layer deposited on top of $Cu(III\text{-}IV)_2$ absorbers [1]. However the toxic hazards related with the use of Cd has triggered the need to look for a Cd-free buffer layer in recent times [2]. Among various alternative candidates, ZnS is considered as one of the most promising materials [3]. ZnS is non-toxic, abundant and cheap. It is a direct wide bandgap n-type compound semiconductor having a bandgap of 3.2 - 3.9eV at room temperature which is higher in comparison with CdS having a bandgap of 2.45eV. The wider bandgap of ZnS enables high energy incident photons to reach the window-absorber junction, enhancing the blue response of the photovoltaic cells and thus contributes to a better cell performance [4]. The efficiency of heterojunction solar cells depend largely on the interfacial properties between absorber and buffer layers. ZnS has the ability to provide better lattice matching with $Cu(III\text{-}IV)_2$ absorbers [1,5].

* Corresponding author: nowshad@eng.ukm.my

Several growth techniques for preparing ZnS thin films have been reported in the literature. These are Chemical Bath Deposition (CBD) [6], Metal Organic Chemical Vapour Deposition (MOCVD) [7], Molecular Beam Epitaxy (MBE) [8], RF Magnetron Sputtering [4], Thermal Evaporation [9] etc.

Magnetron sputtering technique has some advantages compared to the other methods such as easier controllability of the deposition parameters, high film growth rate, relatively cost-effective and specially for the compatibility with the sputtering depositions of $Cu(III\text{-}IV)_2$ absorbers and window layers, leading to a development of a full in-line sputtering technique [1,3].

In this work, we have deposited ZnS thin films by RF magnetron sputtering. The deposition was done at room temperature. Post deposition annealing treatment of the grown films was carried out to investigate the effect of different annealing temperatures on the structural, topographical, optical and electrical properties of the films in order to optimize the growth.

2. Experimental

Soda lime glass substrates were cleaned in ultra-sonic bath, degreased by methanol-acetone-methanol and deionised water for 5 minutes, respectively. Then, the cleaned glasses were dried by dry N_2. The samples were immediately loaded into the RF-sputtering chamber after cleaning. Before the start of sputtering, the chamber pressure was pumped down to a base pressure of 5.8×10^{-5} Torr. Pre-sputtering for 5 minutes was carried out in order to remove the target surface contamination. Then, the main deposition of ZnS was performed with a pure argon gas flow rate of 5 SCCM, RF power of 80W, and a working pressure of 4.0×10^{-2} Torr. The substrate temperature was maintained at room temperature during the deposition for 90 minutes. To study the effect of different annealing temperatures, the as-deposited films were annealed in a vacuum furnace at 300˚C, 400˚C & 500˚C, respectively. The annealing treatment was carried out for 40 minutes. The chamber pressure was maintained in the range of 80-100 mTorr, by a continuous evacuation through a mechanical roughing pump. Upon completion of annealing, the samples were left in the annealing chamber for natural cooling until the temperature reached the room temperature.

The structural and crystallographic properties of the films were observed from the X-ray diffraction (XRD) data taken by 'BRUKER aXS-D8 Advance Cu-Kα' diffractometer. The XRD patterns were obtained in the 2θ ranging from 20˚ to 60˚ using Cu-Kα radiation of wavelength, λ = 1.5408 Å. The surface topography and roughness of the films were found by 'NANOSURF EASYSCAN 2' AFM (Atomic Force Microscopy). The optical properties like transmission, absorption and optical energy band gap of the films were studied by the 'Lambda 900 UV/Vis/NIR' spectrometer. The electrical properties such as, carrier concentration, mobility, resistivity and Hall coefficients were measured by Hall Effect measurement tool 'ECOPIA 3000'.

3. Results and discussions

3.1 Structural Analysis by XRD:

X-ray diffraction patterns were analysed in order to determine the structural and crystallographic properties. Fig. 1 shows the XRD patterns found for the as deposited and annealed ZnS thin films. The effect of annealing is vividly visible from the obtained XRD spectra as no significant peaks were observed for the as-grown films depicting an amorphous nature. However, for the different temperature annealed films, only one significant peak at $2\theta = 28.88^{\circ}$ were observed to appear corresponding to the $(111)^{cub}$ reflection plane and exhibited a cubic or zinc blende (JCPDS Card: 01-080-0020) structure. Only one significant peak for the annealed films indicated that the films are of a single crystalline structure and the planes are parallel to the substrate surface [2]. The 500˚C and 300˚C annealed films possessed higher intensity indicating the best preferential oriented structures.

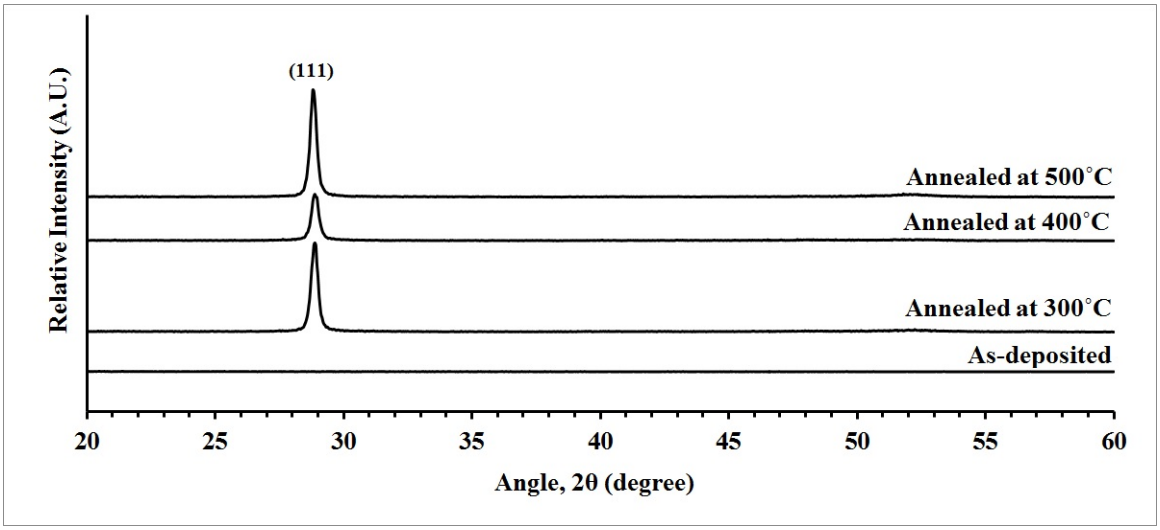

Fig. 1. XRD Spectra of as-deposited and annealed ZnS thin films.

The lattice constant 'a' for cubic phase structure [hkl] for the films has been calculated from the Brag's law and Vegard's law [10, 11].

$$d_{hkl} = (\lambda/2)\ \mathrm{cosec}\theta \quad (1)$$

$$a_{cubic} = d_{hkl}\ (h^2+k^2+l^2)^{1/2} \quad (2)$$

where, d is the interspacing between the planes in the atomic lattice, λ is the X-ray wavelength (0.15406 nm), θ is the angle between the incident ray and scattering planes and a is the lattice constant.

For obtaining more structural information, the mean crystallite sizes (D) of the films are calculated using Scherrer equation [12]:

$$D_{hkl} = 0.9\lambda/(\beta\cos\theta) \quad (3)$$

where, λ is the X-ray wavelength (0.15406 nm), θ is the Bragg diffraction angle and β is the full width at half maximum [FWHM] of the film diffraction peak at 2θ. Crystallinity is highly related to FWHM values. The higher FWHM values of the films indicate the deterioration of the crystallinity, whereas the larger crystallite sizes signify the improved crystallinity of the films [3,4]. The calculated values for different structural parameters of the as grown and annealed ZnS thin films are shown in Table 1. The FWHM values for 300˚C, 400˚C and 500˚C annealed films are found as 0.32, 0.36 and 0.24, respectively along the (111) phase and the mean crystallite sizes of the films were about 25.57, 22.74 and 34.08 nm, respectively. This indicates better crystallinity for the highest temperature annealed films and also satisfies with the highest peak intensity clearly seen from the XRD spectra. Valenzuela and Russer reported that, the FWHM of an XRD peak is reliant on the crystallite size and the lattice strain caused by the defect and/or dislocations [13].
The development of lattice strain is caused by varying displacement of the atoms with respect to their reference-lattice positions. In other words, the origin of microstarin is related to lattice 'misfit', which actually depends upon the deposition condition of the films. The developed microstrain (ε) is calculated from the relation [14,15].

$$\varepsilon = (\beta/4)\ \tan\theta \quad (4)$$

where, β and θ has their usual significances. The lower value of ε indicates single crystalline nature of the films. Highly polycrystalline films will show a larger value of ε indicating more strain on the lattice. The derived values for the microstrain is smaller compared to other

microstrain values for polycrystalline nature films found in the literature [4], confirming the single crystalline nature of the films.

Finding the dislocation density of thin films is crucial for studying the crystallographic properties of thin films. Dislocation is basically imperfection in a crystal caused by the miss registry of the lattice in one part of the crystal with respect to another part. It is not an equilibrium imperfection, as it may occur randomly. The dislocation density of thin films is calculated by the Williamson and Smallman's relation [16].

$$\delta = n / D^2 \tag{5}$$

where, n is a factor, which is considered almost equal to unity for minimum dislocation density and D is the crystallite size or grain size. The calculated microstrain and dislocation density values are given in Table 1.

Table I. Calculated Values of the structural parameters of ZnS thin films.

Sample Type	**hkl**	**d_{hkl} (nm)**	**a (Å)**	**β (deg)**	**D_{hkl} (nm)**	**ε (10^{-3})**	**δ (10^{11} cm^{-2})**
As-grown	-	-	-	-	-	-	-
300˚C annealed	(111) C	0.309	3.09	0.32	25.57	0.36	1.53
400˚C annealed	(111) C	0.307	5.30	0.36	22.74	0.41	1.93
500˚C annealed	(111) C	0.309	5.40	0.24	34.08	0.27	0.86

3.2 Surface topography analysis by AFM:

The surface topographical studies of the as-deposited and annealed thin films were examined with the help of Atomic Force Microscopy (AFM) and are shown in Fig. 2. The calculated average roughness (s_a) and RMS roughness (s_q) values are recorded and the roughness trend is plotted in Fig. 3 for all the films. The effect of annealing can be observed from the roughness values as both s_a and s_q has decreased after annealing. Since the sputtering deposition was carried out in room temperature, there was no additional thermal energy to facilitate the crystallization. But after the post deposition annealing treatment, the applied thermal energy has played a role in the crystallization of the films and resulting more smoother surface. From the image of the as-deposited film it is observed that, the grains are smaller in size with an uneven distribution and random orientation along the surface. Whereas, from the image of the annealed film it is clearly visible that, the grains have become more closely packed, evenly distributed hence reducing the roughness of the films. An increase in the overall grain size can also be observed in this case. The results agreed well with the XRD patterns.

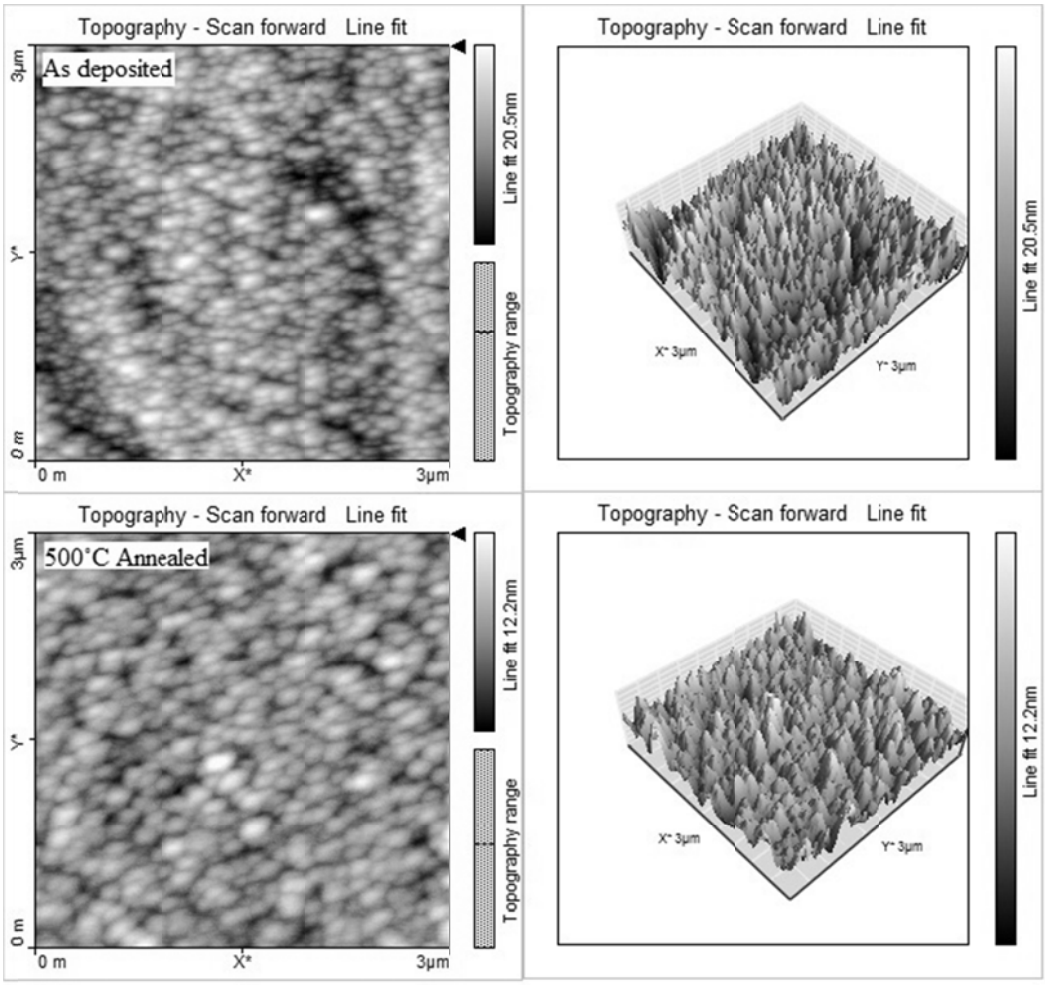

Fig. 2. 2D and 3D AFM images for the as-deposited and annealed ZnS thin films.

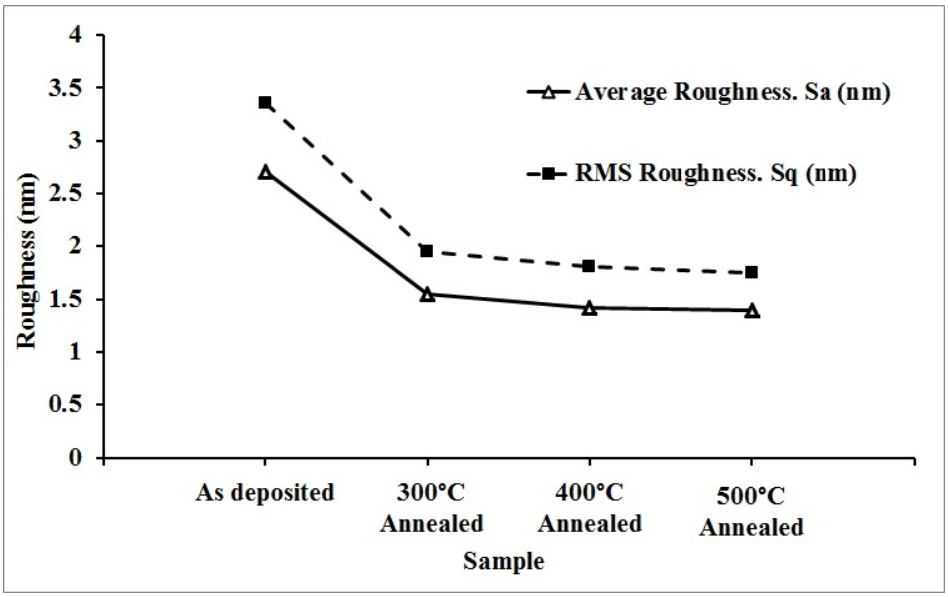

Fig. 3. Average roughness and RMS roughness for the as-deposited and annealed ZnS thin films.

3.3 Optical Properties from Spectroscopy:

The optical properties such as transmission, absorption and optical bandgap are usually examined by UV-Vis spectrometry. During the scanning process, a commercially used blank soda lime glass slide was placed in one of the beam directions and another glass containing the deposited layer of ZnS was placed in the second beam direction. The data for transmission and absorption spectra ranging from 300 to 900 nm were obtained in this fashion. The transmittance spectra for the grown and annealed films are shown in Fig. 4. The films exhibit an average transmittance of 85% along the range, confirming the suitability of the films to be used as a buffer layer in photovoltaic applications.

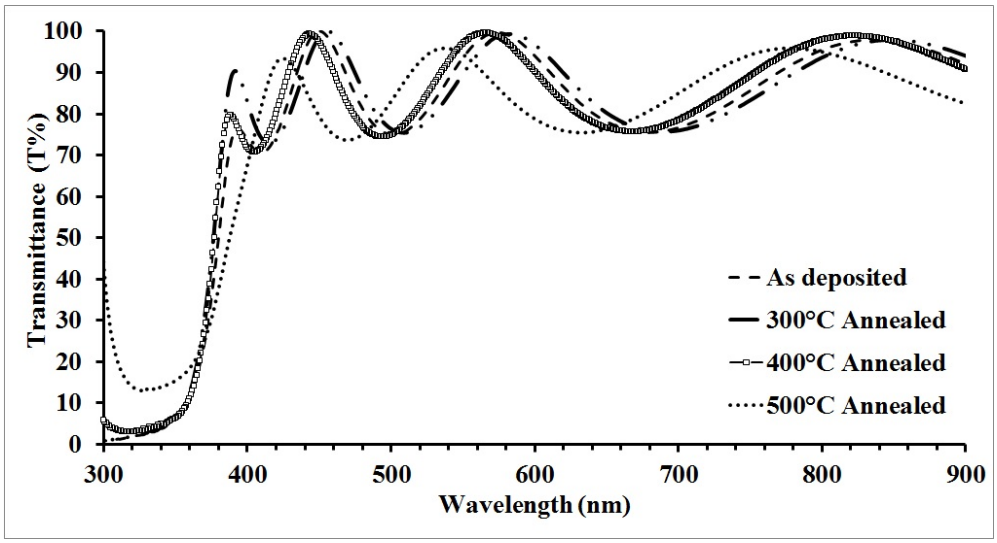

Fig. 4. Transmittance vs. wavelength spectra of as-deposited and annealed ZnS thin films.

The bandgaps of the as-deposited and annealed films were calculated from the following relationship [17].

$$\alpha = A(h\upsilon - E_g)^{1/2} / h\upsilon \quad (6)$$

where, α is the absorption coefficient; A is a constant; $h\upsilon$ is the energy of incident photon and E_g is the bandgap. The plot of $(\alpha h\upsilon)^2$ versus $h\upsilon$ for the films are shown in Fig. 5. The bandgap energy is obtained by extrapolating the straight line portion of the graph to zero absorption coefficients. The intercept on the energy axis indicates the value of band gap energy [18]. From Fig. 5, the bandgap of the as-deposited films are found to be 3.24 eV. After annealing at 300˚C the band gap red shifted to 3.29 eV. However further annealing caused a blue shift in the band gap from 3.29 eV to 3.19 eV. These results indicate that annealing to a certain limit can increase the bandgap, and it starts to decrease then.

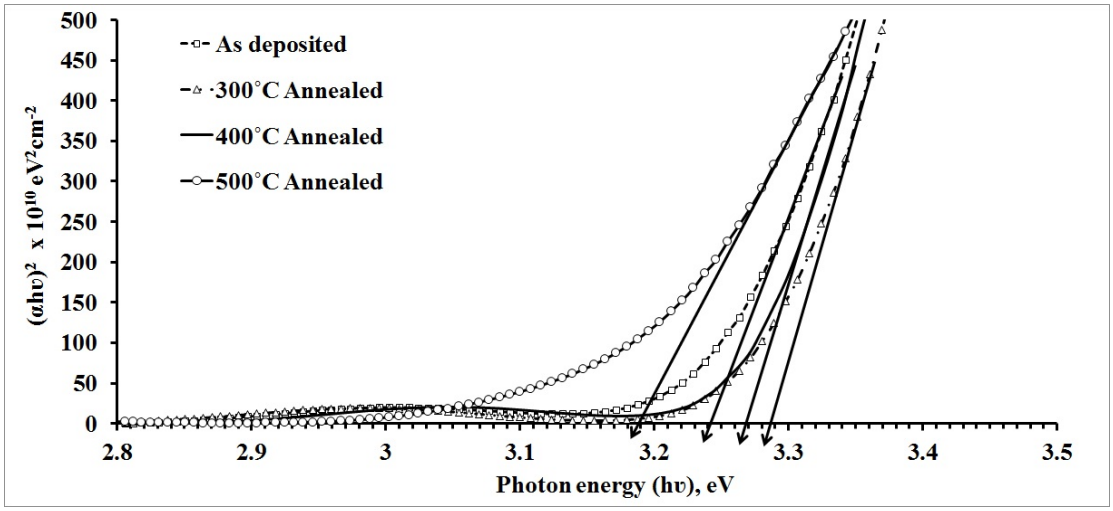

Fig. 5. Plot of $(\alpha h\upsilon)^2$ vs. photon energy ($h\upsilon$) for as-deposited and annealed ZnS thin films.

3.4 Electrical Characterization

The electrical properties of the as-deposited and annealed ZnS thin films were analysed at room temperature by resistivity and Hall Effect measurements with an integrated resisitivity / Hall measurement system (ECOPIA 3000).

All samples exhibit n-type conductivity regardless of heat treatment. The bulk carrier density, mobility, resistivity and Hall coefficients found from the Hall Effect measurements are represented in Table 2. Each bulk carrier density is in the order of 10^{12} cm^{-3}. The maximum value of carrier concentration and mobility is observed with the value of 8.56 x 10^{12} cm^{-3} and 23.5 x 10^{1} cm^2/Vs, respectively resulting an improvement of conductivity for the highest temperature (500˚C) annealed films. This improvement of conductivity can be attributed to the increase in the carrier concentration and mobility. Fig. 6 shows the change of bulk carrier density and resistivity of the as-deposited and annealed ZnS thin films. The maximum resistivity of 2.98 x 10^4 Ω cm is noted for the films annealed at 300˚C and the resistivity values has shown a decreasing trend with the increment of annealing temperature, indicating the semiconducting nature of the films [19]. This decrement of resistivity can be correlated with the XRD results, as it is evident from the literature that, higher degree of crystallinity can lead to lower resistivity of the films [20]. In this study, the highest XRD peak was recorded for the 500˚C temperature annealed films, and they are showing minimum resistivity values of 3.1 x 10^3 Ω cm.

Table II. Electrical Properties of as-deposited and annealed ZnS thin films.

Sample	Bulk Concentration [x 10^{12}] (cm^{-3})	Conductivity [x 10^{-5}] (Ω^{-1} cm^{-1})	Mobility [x 10^{1}] (cm^2/Vs)	Resistivity [x 10^{4}] (Ω cm)	Hall Co-efficient [x 10^{5}] (cm^3/C)
As-deposited	5.54	5.77	6.51	1.73	11.3
Annealed at 300˚C	7.26	3.35	2.88	2.98	8.60
Annealed at 400˚C	4.20	5.92	8.80	1.69	14.9
Annealed at 500˚C	8.56	32.3	23.5	0.31	7.28

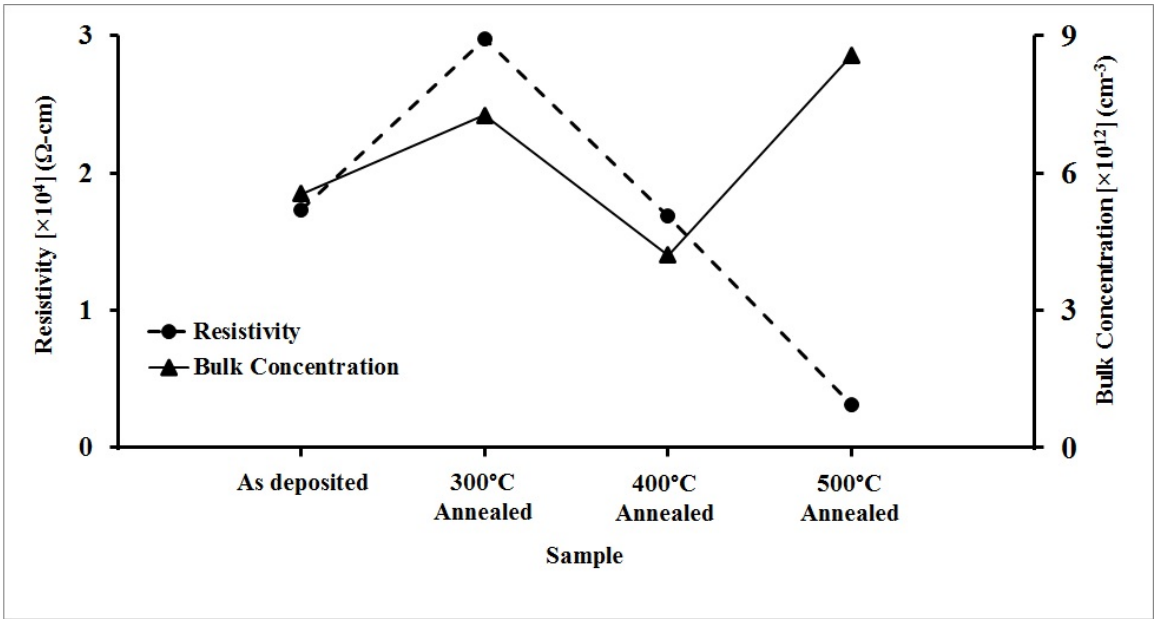

Fig. 6. Variation of Resistivity and Bulk Concentration of the as-deposited and annealed ZnS thin films.

4. Conclusion

The structural, optical and electrical properties of the as-deposited and annealed ZnS thin films have been studied through XRD, AFM, UV-Vis spectrometry and Hall Effect measurement. The effects of annealing has been significant as the sputtered as-grown films in room temperature exhibit an amorphous nature, whereas the annealed films have shown crystalline nature of the zinc-blende structure with a (111) preferential orientation. For the maximum temperature annealed films, crystallite size was found to be the highest along with lowest microstrain and dislocation density values ensuring the better crystallinity as compared to others. The surface roughness gradually decreased with the increase of annealing temperature. The overall average transmittance of 85 % is found for all the films. The bandgap has been found to be 3.24 eV for the as-deposited films, whereas after annealing it increased to 3.29 eV, proving the potential to be used as a buffer layer in thin film solar cells. The minimum resistivity is found for the 500˚C temperature annealed films with the highest bulk carrier concentration of the order of 10^{12} cm^{-3}, which is in good agreement with the XRD results.

Acknowledgment

This work is supported by the Department of Electrical, Electronic & Systems Engineering and Solar Energy Research Institute (SERI) of The National University of Malaysia through the Ministry of Higher Education research grant with codes FRGS/1/2013/TK07/UKM/01/3 and ERGS/1/2012/TK07/UKM/01/4. Appreciations are also extended to the Solar Energy Research Institute (SERI), The National University of Malaysia and the VP unit of King Saud University (KSU) of Saudi Arabia.

References

[1] Le-Xi Shao, Kuen-Huei Chang, Huey-Liang Hwang, Applied Surface Science **212-213**, 305 (2003).
[2] Z. Limei, X. Yuzhi, L.I. Jianfeng, Journal of Environmental Sciences Supplement: pp. 76-79 (2009).

[3] D. H. Hwang, J. H. Ahn, K. N. Hui, K. S. Hui Y. G. Son, Nanoscale Res Lett. **7**(1), 26 (2012).
[4] M. A. Islam, M. S. Hossain, M. M. Aliyu, Y. Sulaiman, M. R. Karim, K. Sopian N. Amin, "Comparative study of ZnS thin films grown by chemical bath deposition and magnetron sputtering", 7th International Conference on Electrical and Computer Engineering, Dhaka, Bangladesh, 2012.
[5] S. W. Shin, S. R. Kang, J. H. Yun, A.V. Moholkar, Jong-Ha Moon, J. Y. Lee, J. H. Kim, Solar Energy Materials & Solar Cells **95**, 970 (2009).
[6] S. Tec-Yam, J. Rojas, V. Rejon, A.I. Oliva, Materials Chemistry and Physics **136,** 386 (2012).
[7] S. Takata, T. Minami, T. Miyata, H. Nanto, J Cryst Growth **86,** 257 (1988).
[8] M. M. Islam, S. Ishizuka, A. Yamada, K. Sakurai, S. Niki, T. Sakurai, K. Akimoto, Solar Energy Materials & Solar Cells **93,** 856 (2011).
[9] M. R. A. Bhuiyan, M. M. Alam, M. A. Momin, Turk J Phys **34,** 43 (2010).
[10] M.A. Islam, M.S. Hossain, M.M. Aliyu, M.R. Karim , T. Razykov, K. Sopian, N. Amin, Thin Solid Films **546,** 367 (2013).
[11] W. L. Roth in M. Aven, J. S. Prener (eds), Physics and Chemistry of II-VI Compounds, North-Holland Publishing Co., Amstredam, pp. 124, 1967
[12] K.S. Rahman, F. Haque, N.A. Khan, M.A. Islam, M.M. Alam, Z.A. Alothman, K. Sopian, N. Amin, Chalcogenide Letters **11**(3), 129 (2014).
[13] A. A. Valenzuela, P Russer, Appl Phys Lett, **55**, 1029 (1989)
[14] K. Sarmah, R. Sarma, H. L. Das, Chalcogenide Letters **5**(8), 153 (2008).
[15] M.A. Islam, M.S. Hossain, M. M. Aliyu, J. Husna, M. R. Karim, K. Sopian, N. Amin, 38 PVSC, Austin, USA, 2012.
[16] M.A. Islam, Q. Huda, M.S. Hossain, M.M. Aliyu, M.R. Karim, K. Sopian, N. Amin, Current Applied Physics **13**, S115 (2013).
[17] J Tauc, Amorphous and Liquid Semiconductors, Plenum Press, New York, 1974.
[18] R. Mariappan, V. Ponnuswamy, M. Ragavendar, D. Krishnamoorthi, C. Sankar, Optik **123**, 1098 (2012).
[19] M.S. Shinde, P.B. Ahirrao, R.S. Patil, , Archives of Applied Science Research **3**(2), 311 (2011).
[20] A.U. Ubale, D.K. Kulkarni, Bulletin Material Science **28**(1), 43 (2005).